Forecasting Research

Forecasting Research Division
Technical Report No. 51

A CASE STUDY OF THE IMPACT OF RADIOSONDE TEMPERATURE AND WIND PROFILES ON MODEL FORECASTS OF A DEVELOPING ATLANTIC DEPRESSION

by
R.J. Graham

May 1993

Meteorological Office
London Road
Bracknell
Berkshire
RG12 2SZ
United Kingdom

Forecasting Research Technical Report No.51

A CASE STUDY OF THE IMPACT OF RADIOSONDE TEMPERATURE AND WIND PROFILES ON MODEL FORECASTS OF A DEVELOPING ATLANTIC DEPRESSION

by

R.J.GRAHAM

Paper to be presented at 13th International Conference on Weather Analysis and Forecasting: Vienna, Virginia, 2-6 August 1993

Forecasting Research Division
Meteorological Office
London Road
Bracknell
Berkshire
RG12 2SZ

May 1993

N.B. This paper has not been published. Permission to quote from it must be obtained from the Assistant Director of the above Met. Office division

A CASE STUDY OF THE IMPACT OF RADIOSONDE TEMPERATURE AND WIND PROFILES ON MODEL FORECASTS OF A DEVELOPING ATLANTIC DEPRESSION

Richard J. Graham

UK Meteorological Office, London Road, Bracknell, UK, RG12 2SZ.

1. INTRODUCTION

The impacts of wind and temperature profiles from Atlantic ship-borne radiosondes on forecasts of a deep depression, which affected the UK on 28 October 1989, are investigated using a series of assimilation/forecast experiments. All experiments comprise data assimilation for 00GMT 27 October followed by a 36hr forecast. The relatively large number of favourably positioned ship ascents available at this time prompted the selection of this case. Of the experiments which show a beneficial impact, one is examined in detail to establish the reason for the observed impact.

The NWP forecast/assimilation model used is the Meteorological Office Unified Model (Cullen, 1993; Lorenc et. al. 1991).

The study forms part of an effort aimed at determining the relative value of wind and temperature profiles to the NWP assimilation/forecast system.

2 CASE DETAILS

The pressure at mean sea level (PMSL), and the 250mb contours and isotachs for the initial time, 00GMT 27 October, are shown in Figs.1a&b. At this time the depression was centred near 45N 15W with a central pressure of 1002mb, and was located on the forward side of a diffluent upper trough. A strong jet stream was present on the western flank of the trough (core strength exceeding 140kn). Over the subsequent 36hrs the depression moved north-eastward and deepened to become located near Dublin at 12GMT 28 October, central pressure 976mb (Fig.1c). A deepening of 20mb occurred during the last 24hrs of the sequence (see Fig.1d).

The 250mb observations from the available ship ascents are shown in Fig.1b and the individual callsigns in Fig.1d. The location of the ships relative to the upper air features suggests a useful division into three groups: **N**, north of the jet stream - C7C and C7L; **C**, central group (sampling the jet core and trough axis) - ONDA, EREU and EREB; **S**, south of the jet stream - DKIW and DKQP.

3. THE IMPACT EXPERIMENTS

The experiments are designed to assess the impact on model forecasts of assimilating selected ship radiosonde data for 00GMT 27 October. Details of the experiments are summarised in Table 1. The CNTL0 and CNTL1 runs represent control experiments. All the ship profiles are withheld from the former, while the latter uses all the available wind and temperature profiles. In run WALL wind profiles only from all ships were used, similarly run TALL uses only temperature profiles. The remaining experiments are named after the profiles assimilated (e.g. WGN - wind profiles from group N). The WGC and TGS profiles were assimilated in run WGCTGS.

The background field (first guess) for all assimilations was obtained by performing 60hrs of "spin-up" assimilation from which all the ship radiosonde data was withheld.

Expt.	Groups used	Temp.&/or wind used	Rms impact (hPa)	Rms error (hPa)	err. red on CNTL0 (%)
CNTL0	None	None	--	6.86	--
CNTL1	All	All	1.62	5.95	13.2
WALL	All	W	0.59	6.39	6.9
TALL	All	T	1.27	6.30	8.2
WGN	N	W	0.18	6.94	- 1.2
TGN	N	T	0.75	6.90	- 0.5
WGC	M	W	0.71	6.28	8.6
TGC	M	T	0.44	6.84	0.4
WGS	S	W	0.26	7.00	- 2.0
TGS	S	T	1.07	6.22	9.4
WGCTGS	M,S	W grp C T grp S	1.73	5.77	15.9

Table 1: Description of forecast experiments; and verification of the t+36 PMSL forecast over the area of Fig.1c. Impact is defined here as rms EXPT-CNTL0.

4. RESULTS

The position and central pressure of the depression from the CNTL0 forecast are marked on Fig.1c and the forecast error is shown in Fig.1e. The forecast position is north-east of the true position and the forecast central pressure 6mb too high. A maximum error of 19mb (too high) is located just west of the low centre. The forecast is clearly poor, and use of the wind and temperature profiles did not correct the gross error in the forecast. Nevertheless some of the profiles did deliver a beneficial impact. The degree of benefit has been measured by the percentage reduction in error on the CNTL0 forecast (far right column, Table 1). The main points of interest in Table 1 are expanded below.

1) Use of temperature profiles alone (TALL) results in a larger error reduction than use of wind profiles alone (WALL).

2) Neither wind nor temperature profiles alone give as large an error reduction as use of both (CNTL1).

3) The largest error reductions derive from the use of temperature profiles from group S south of the jet (TGS), and the use of wind profiles from group C in the jet core and trough axis region (WGC). Because some of the profiles deliver a negative impact, the error reduction achieved by WGC and TGS is greater than when all

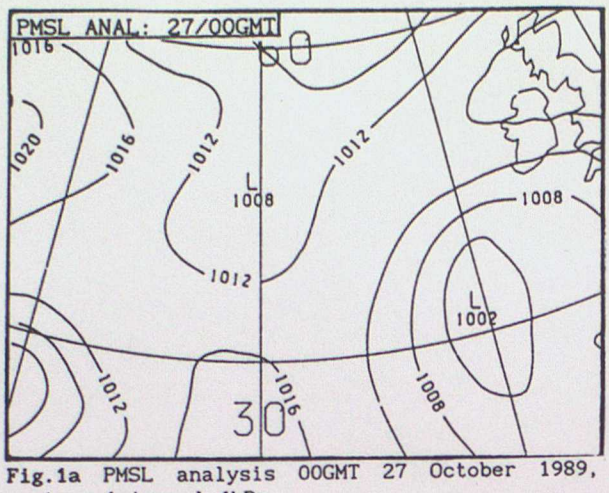

Fig.1a PMSL analysis 00GMT 27 October 1989, contour interval 4hPa.

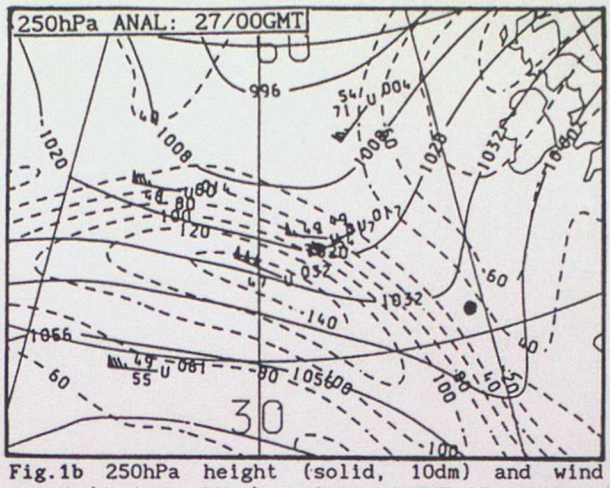

Fig.1b 250hPa height (solid, 10dm) and wind speed (dashed, 20kn) analysis 00GMT 27 October. The low position is marked "•". The 250mb observations from the radiosonde profiles are also shown.

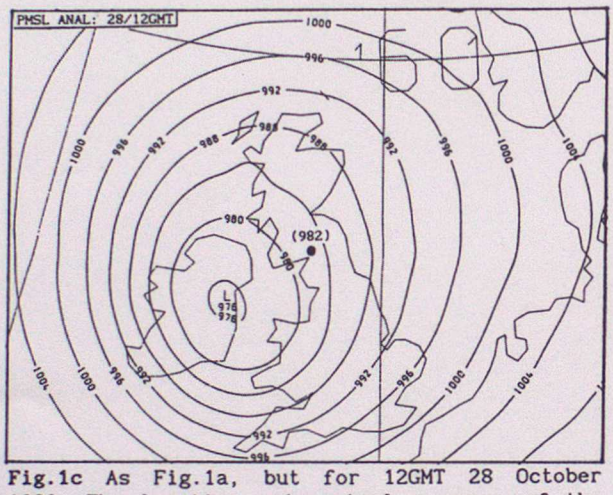

Fig.1c As Fig.1a, but for 12GMT 28 October 1989. The location and central pressure of the low in the CNTL0 forecast have been added.

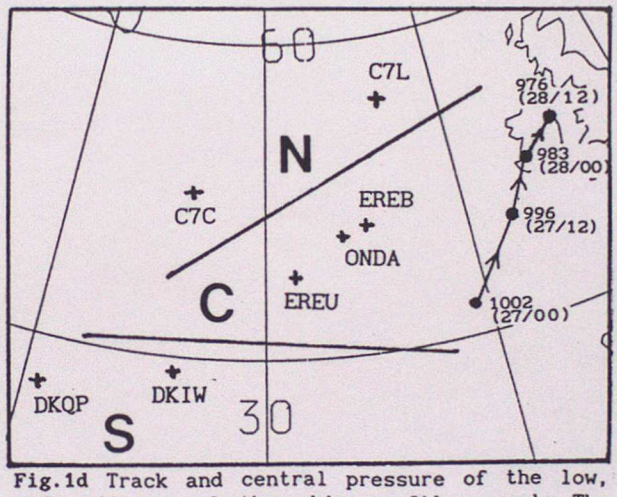

Fig.1d Track and central pressure of the low, and callsign of the ship profiles used. The groups of profiles, N, C, and S used in the experiments are shown.

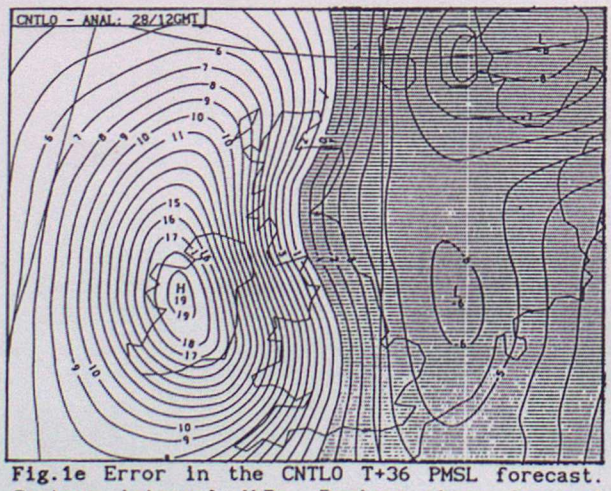

Fig.1e Error in the CNTL0 T+36 PMSL forecast. Contour interval 1hPa. Regions where forecast pressure is too low are shaded.

the temperature or wind profiles are used (TALL, WALL). The impact delivered by the TGS and WGC profiles is shown in Figs.2a&b respectively. The amplitude of the TGS impact is larger than that of WGC, however comparison with Fig.1e shows that the distribution of the impact is superior for the WGC experiment (compare the alignment of the zero impact and zero error contours). Because of the better distribution of impact, the WGC run gives an error reduction comparable with that of the TGS run for a smaller rms impact (see Table 1). Note also that the WALL profiles deliver an error reduction comparable to that of the TALL profiles for a much smaller rms impact. To summarize; temperature profiles deliver the largest rms impact - however, the proportion of the impact which is beneficial is larger when wind profiles are used. Consequently, the error reduction obtained with either wind or temperature profiles is comparable.

4) The error reduction improves from 13.2% for CNTL1 (the operational configuration, i.e. all

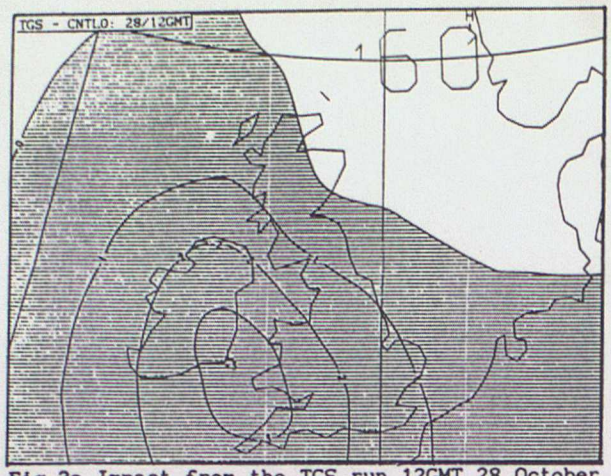

Fig.2a Impact from the TGS run 12GMT 28 October 1989 (TGS t+36 - CNTL0 t+36). Negative differences are shaded.

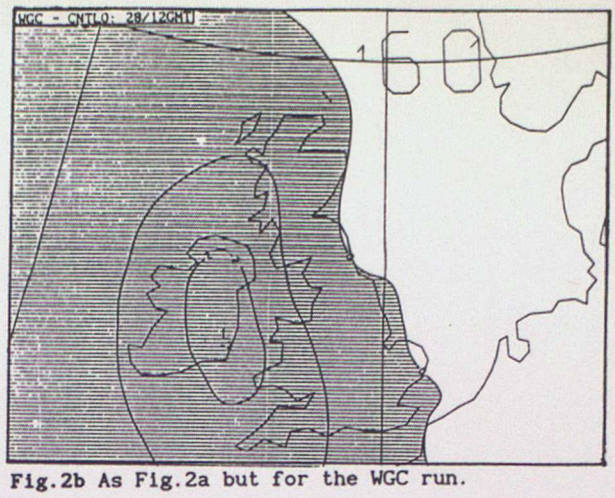

Fig.2b As Fig.2a but for the WGC run.

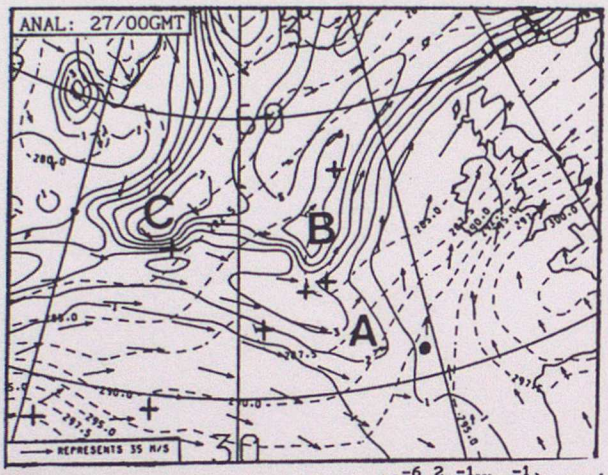

Fig.3a 315K PV (solid, $1\times10^{-6}m^2s^{-1}Kkg^{-1}$) and wind vector analysis with 850mb isentropes (dashed, 2.5K), 00GMT 27 October. Radiosonde positions are marked "+", the low position "•".

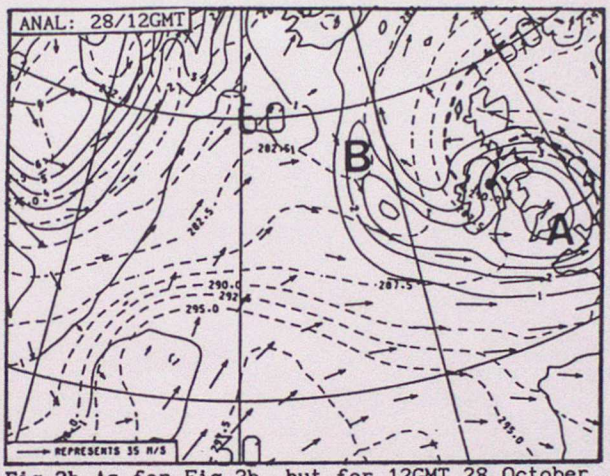

Fig.3b As for Fig.3b, but for 12GMT 28 October. The 290K isentrope has been highlighted.

profiles used) to 15.9% if only the WGC and TGS profiles (run WGCTGS, i.e omitting all profiles which give a negative or small impact).

5. INTERPRETATION OF THE *TGS* AND *WGC* IMPACTS

To interpret the impacts it is helpful to consider the evolution in terms of isentropic potential vorticity (PV) (Hoskins et. al., 1985). The 315K PV field at the initial time, 00GMT 27 October, and at 12GMT 28 October are shown in Figs.3a&b. Examination of intervening charts (not shown) shows that the low develops as the positive anomaly *A* (Fig.3a) moves eastward, intensifies (presumably through latent heat release) and engages the baroclinic zone located over the UK. Distortion of the baroclinic zone produces a low-level warm anomaly and intensification of the low proceeds as "phase locking" between the upper PV anomaly *A* and the low-level warm anomaly is established. By 12GMT 28 October (Fig.3b) a well defined warm ridge has formed over Ireland, the low is located within the apex of this ridge. Anomalies

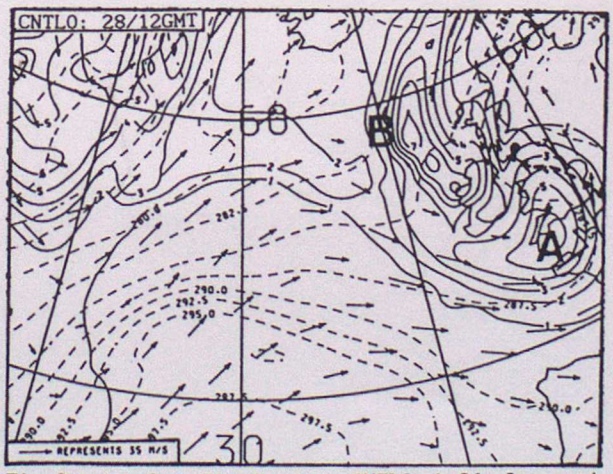

Fig.3c As for Fig.3a but CNTL0 t+36 forecast valid 12GMT 28 October 1989.

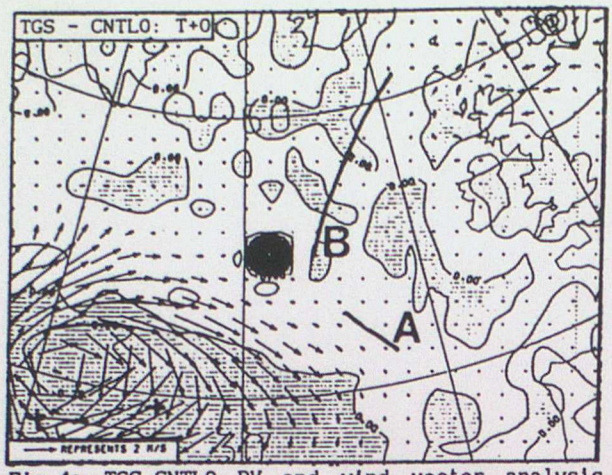

Fig.4a TGS-CNTL0 PV and wind vector analysis differences, 00GMT 27 October 1989. The axis of anomalies *A* and *B* in the CNTL0 run have been added. Units as Fig.3a, contour interval 0.25. Negative PV differences are shaded.

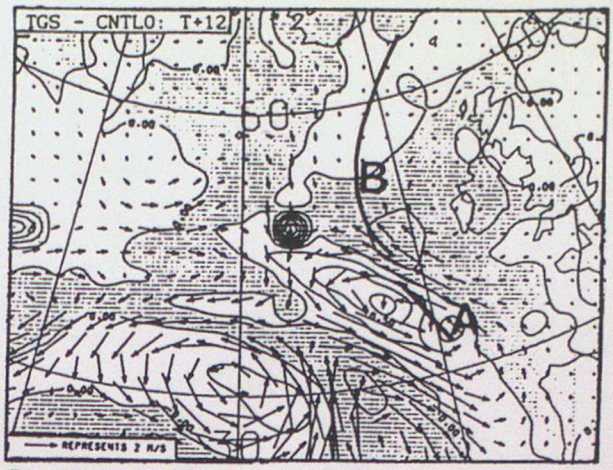

Fig.4b As Fig.4a but for T+12.

B and *C* (Fig.3a) move eastward at first and merge into a single anomaly which by 12GMT 28 has become a minor, slow moving, feature controlled by the flow induced by *A*.

The corresponding chart from the CNTL0 forecast, valid 12GMT 28 October, is shown in Fig.3c. Comparison with Fig.3b shows that in the CNTL0 forecast anomaly *B* has moved further eastward, and is competing with anomaly *A* for "phase locking" with the low-level thermal ridge. Consequently the low-level warm ridge is less well defined than in the actual evolution and is located north-east of the true position. This is consistent with a weaker surface depression located north-east of the actual position (ref Fig.1c).

From the above discussion it is reasonable to assume that for assimilation of the temperature or wind profiles to result in an improved forecast, they must have the effect of weakening anomaly *B*, and/or slowing its eastward progression, and strengthening anomaly *A*. Consistent with the above, comparison of the WGC and CNTL0 analyses showed that use of wind profiles in the trough axis and jet core resulted in anomaly *B* being positioned further west and in anomaly *A* being strengthened slightly. These effects were maintained into the forecast.

In contrast the TGS profiles cannot have a direct impact on the analysis of *A* and *B* since they are situated some distance upstream. In this case the evolution of *A* and *B* is improved by the downstream propagation of information during the forecast. This may be confirmed by reference to Figs.4a&b which show differences between the TGS run and the CNTL0 run at T+0 and T+12. The differences at T+0 take the form of an increase in anticyclonic circulation associated with negative PV differences near 45N 42W. - there is very little difference in the PV field in the vicinity of anomalies *A* and *B* (the grid point noise near the centre of the chart is a numerical artefact and should be ignored). By T+12, however, a train of positive and negative differences has formed which has the desired effect of strengthening anomaly *A* and weakening anomaly *B*.

6. CONCLUSIONS

In the case studied, profiles of wind and temperature are shown to have a comparable beneficial impact on the forecast. The benefit delivered by the temperature profiles is slightly larger in an rms sense, however, there is evidence that the wind profiles give a better areal distribution of the impact. Most of the impact derives from two temperature profiles south of the jet stream and three wind profiles which sampled the jet core and trough axis. Use of temperature profiles within the trough axis and jet core had very little impact. This would seem to confirm the expectation that where analysis of the vorticity field is crucial, wind profiles are more useful that temperature profiles.

The TGS experiment illustrates the fact that data impacts on a particular system may derive from regions remote from the system at the initial time.

The results of the study are limited by a number of factors. In particular, the specific character of the case study makes it difficult to draw general conclusions. In addition, we have not considered the impact of observation errors, or the dependence of the results on analysis technique (see Appendix). Furthermore, the sparse distribution of the ship data used means that the results are unlikely to be typical of the impacts delivered by satellite-based wind and temperature profiles. In future work it is hoped to address these limitations through more wide ranging studies using simulated wind and temperature profiles.

References

Cullen, M.J.P., 1993: The Unified Forecast/Climate Model. *Meteorol. Mag.*, **122**, No.1449, 81-93

Hoskins, B.J., McIntyre, M.E. and Robertson, A.W., 1985: On the use and significance of isentropic potential vorticity maps. *Quart. J. Roy. Meteor. Soc.*, **111**, 877-946

Lorenc, A.C., Bell. R.S. and Macpherson, 1991: The Meteorological Office Analysis Correction data assimilation scheme. *Quart. J. Roy. Meteor. Soc.*, **177**, 59-89

APPENDIX

Impact of wind and temperature profiles on the 250hPa wind analyses

The analysis scheme allows temperature observations to have a direct impact on the wind analysis through the use of geostrophic wind increments derived from the temperature analysis increments. However, in the version of the scheme used for this study, the converse was not the case, i.e. no temperature (mass) increments were derived from the wind increments. This inequality in the use of wind and temperature data might be expected to be a contributing cause of the slightly greater impact found for temperature profiles. However, evidence from the TGC and WGC experiments, discussed below, suggests that temperature and wind data may give conflicting signals about the sense of the wind field, and in such cases uses of geostrophic wind increments will tend to degrade the wind analysis.

Figs.5a&b show the WGC-CNTL0 and TGC-CNTL0 250hPa vector wind differences, respectively. Reference to Fig.5a shows that use of wind profiles (at the three ship locations shown) leads to more cyclonic flow in the WGC analyses relative to the CNTL0 analysis. The TGC wind differences are shown in Fig.5b and arise from two factors; the use of geostrophic wind increments, and the dynamical adjustment of the wind field to the temperature data during the assimilation. In contrast to the WGC run, the differences in the TGC run have an anticyclonic sense and are much broader in scale, with little influence in the immediate vicinity of the three profiles. Clearly, the wind differences bear little resemblance to those obtained with use of wind profiles (Fig.5a), and in this case we may conclude that use of the temperature profiles has damaged the wind analysis.

The corresponding WGC-CNTL0 and TGC-CNTL0 height differences are shown in Figs.6a&b, respectively. In the WGC experiment the contour trough is deepened relative to CNTL0 with negative differences peaking over a region centred on the middle profile to the west of the upper trough. This is consistent with the results of section 5 where it is shown that the impact of the wind profiles was to move the analysed position of the trough westward. In the TGC experiment (Fig.6b), the height field differences are positive, as is consistent with the anticyclonic sense of the wind differences of Fig.5b, and act to fill the trough relative to CNTL0.

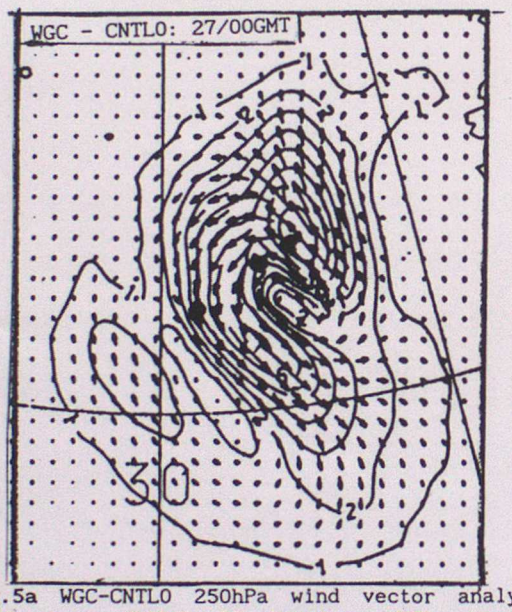

Fig.5a WGC-CNTL0 250hPa wind vector analysis differences 00GMT 27 October 1989. Contour interval 1kn. The locations of the WGC and TGC profiles are shown.

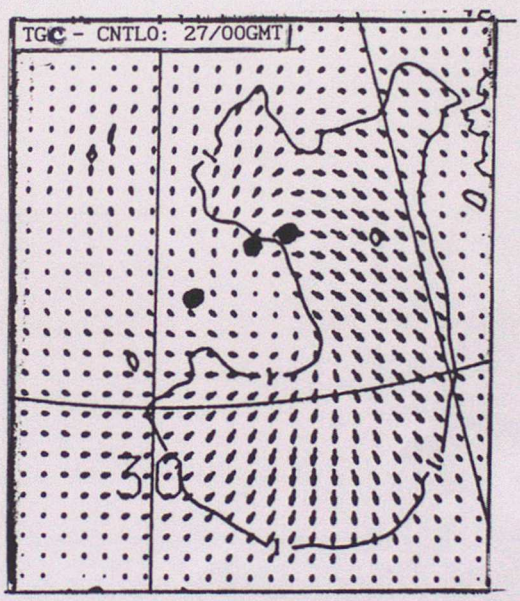

Fig.5b As Fig.5a but TGC-CNTL0.

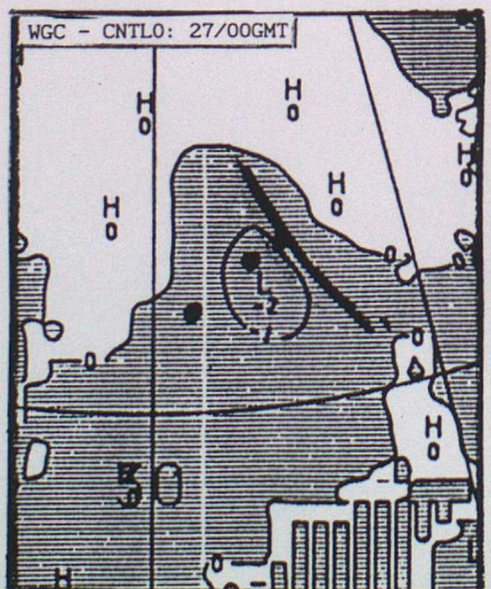

Fig.6a WGC-CNTL0 250hPa height differences 00GMT 27 October. Contour interval 1dm. The axis of the upper trough is shown. The locations of the WGC and TGC profiles are shown.

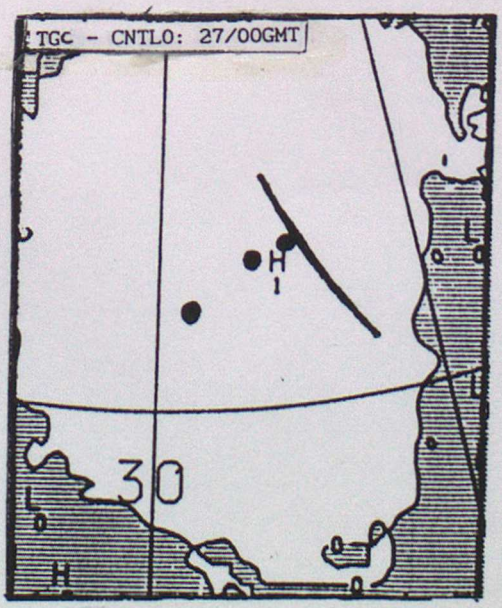

Fig.6b As Fig.6a but TGC-CNTL0.